Biosensors and Bioelectronics 40 (2013) 186–192

Contents lists available at SciVerse ScienceDirect

Biosensors and Bioelectronics

journal homepage: www.elsevier.com/locate/bios

Real time monitoring of thrombin interactions with its aptamers: Insights into the sandwich complex formation

Camille Daniel, Feriel Mélaïne, Yoann Roupioz [1], Thierry Livache, Arnaud Buhot *

SPrAM (UMR 5819: CEA, CNRS, UJF), INAC, CEA Grenoble, 17 rue des Martyrs, 38054 Grenoble cedex 9, France

ARTICLE INFO

Available online 21 July 2012

Keywords:
Thrombin aptamer
Sandwich complex formation
Surface plasmon resonance imaging
Real time monitoring

ABSTRACT

Aptamers are raising an increasing interest for biosensor applications as replacements for antibodies due to their high stability and low cost. Thrombin, a key enzyme in the coagulation cascade, is an archetypical target against which two different aptamers, binding to two different exosites, have been selected. Recent studies dedicated to thrombin monitoring applications of biosensors have taken advantage of a potential sandwich-like structure between thrombin and these two aptamers for amplification purposes. However, in most cases, only end-point analysis was observed as a result of labeling requirements, thus preventing access to the kinetics of the complex formation. By using Surface Plasmon Resonance (SPR) imaging of aptamer-functionalized biosensors, we followed the binding of thrombin on the sensor and its interaction with a second reporter aptamer in real-time and in a label-free manner. Surprisingly, we showed that the injection of a second unlabeled-aptamer following the previous thrombin injection destabilized the thrombin–aptamer complex formed on the sensor surface, thus limiting any further amplification. However, the direct co-injection of thrombin, pre-complexed with a biotinylated aptamer bound to streptavidin efficiently increased the SPR signal by comparison to single thrombin detection. The various injection sequences performed may be rationalized considering a poor selectivity of one of the aptamers towards its exosite and a further negative allosteric effect upon sandwich complexation of the thrombin with its aptamers.

1. Introduction

Aptamers are small nucleic acids selected by SELEX (systematic evolution of ligands by exponential enrichment) procedure for their high affinity to target molecules (Ellington and Szostak, 1990; Tuerk and Gold, 1990). Besides their use as therapeutic agents, they recently appeared as an interesting alternative to antibodies in sensor and diagnostic assay applications (Jayasena, 1999; Sassolas et al., 2011; Tombelli et al., 2005). The principal advantages reside in their low cost, easy synthesis, chemical stability, versatility and potential large-scale production. Due to multiple implications in the coagulation process (Lane et al., 2005), thrombin was the first protein targeted for single-stranded DNA aptamer selection (Bock et al., 1992). This protein presents two exosites I and II, one for the binding of fibrinogen and the other for heparin, which are also the binding sites of 15-mer (APT1) and 29-mer (APT2) aptamers, respectively (Bock et al., 1992; Tasset and Kubik, 1997). Interestingly, a wide range of K_D have been published for the binding of both Bocks' and Tassets' aptamers: from 1.2 nM to up to 200 nM and 0.5 nM to 255 nM, respectively (Ahmad et al., 2011; Bock et al., 1992; Li Y. et al., 2008; Tasset and Kubik, 1997). This wide range of data collected from different techniques emphasizes the difficulty for reliably assessing the thermodynamic parameters of the aptamer interactions with thrombin.

On one hand, many studies on thrombin-sensitive biosensors have taken advantage of the possible sandwich complex formation between thrombin and the two aptamers for amplification purposes by electrochemical (Bai et al., 2011) or fluorescence readout (Tennico et al., 2010), enzymatic catalysis (Centi et al., 2007) and Streptavidin (Tang et al., 2007) or nanoparticle coupling (Chen et al., 2010; Kwon et al., 2012; Wang et al., 2011). All previous sandwich-based aptamer assays on thrombin require the labeling of the reporter aptamer. Surprisingly, unlabeled sandwich build-up did not yield any signal amplification by Surface Plasmon Resonance (SPR) detection (Tang et al., 2007). Additionally, in most sandwich-based thrombin detection, only final end-point results are attainable – due to the reporter detection brought by the second binding aptamer – thus preventing any access to the real-time kinetics data for the sandwich construction. On the other hand, binding of natural ligands on exosites I or II of thrombin have been known for long time for having multiple allosteric effects upon the enzymatic activity of thrombin (Fredenburgh et al., 1997; Verhamme et al., 2002), whereas allosteric effects of aptamer binding on thrombin exosites have only poorly been studied (Olmsted et al., 2011). In this

* Corresponding author. Tel.: +33 438 78 38 68.
E-mail addresses: yoann.roupioz@cea.fr (Y. Roupioz), arnaud.buhot@cea.fr (A. Buhot).
[1] Tel.: +33 438 78 98 79; fax: +33 438 78 56 91.

0956-5663/$ - see front matter © 2012 Elsevier B.V. All rights reserved.
http://dx.doi.org/10.1016/j.bios.2012.07.016

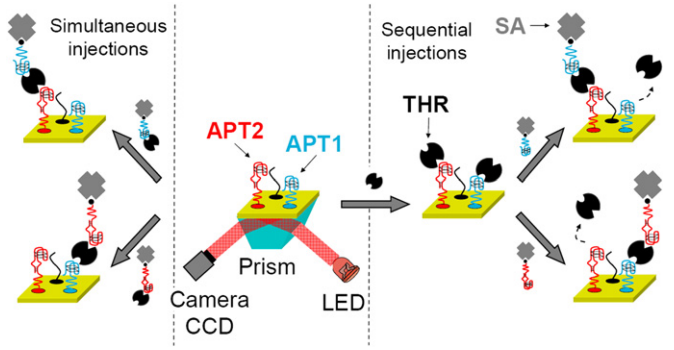

Scheme 1. General scheme of the various protocols for sample injections led on the biosensor. The microarray is functionalized with each aptamer (APT1 and APT2) along with negative controls (APT1c and APT2c, complementary sequences to the aptamers). Molecular interactions occurring on the biosensor surface are monitored in real-time by Surface Plasmon Resonance imaging. Two different strategies have been tested for sandwich complex formation between thrombin and aptamers: sequential vs simultaneous injections.

paper, we aim to evaluate the kinetics of each molecular interactions of both aptamers with thrombin and thereby determine possible allosteric effects and the ideal sandwich strategy for signal amplification by monitoring the sequential or simultaneous injections in real-time.

For this purpose, we developed a DNA microarray functionalised with both aptamers and control oligonucleotides and followed the sandwich construction in real time by Surface Plasmon Resonance imaging (SPRi). Several sample injection series (see Supplementary Data, Appendix A) were assayed to gain better insights into the molecular interactions and then assess the best amplification strategy (Scheme 1). Surprisingly, we found that the pre-complexation of thrombin with an aptamer in solution or grafted on the sensor yielded contradictory effects for signal amplification. The injection of a second reporter aptamer destabilized the preformed complex thrombin–aptamer on the microarray whatever the aptamer couples suggesting negative allosteric effects upon sandwich formation. Furthermore, strong evidences of poor selectivity of APT1 towards thrombin exosites suggest the injection of pre-complexed thrombin with APT2 on grafted APT1 is the best strategy for signal amplification.

2. Materials and methods

2.1. Reagents and chemicals

Human alpha-thrombin (THR) was purchased from Haematologic Technologies Inc. (Essex Junction, VT, USA). Bovine serum albumin (BSA), cytochrome c (cyt c), streptavidine (SA), 11-mercapto-undecanoic acid, *N,N′*-dicyclohexylcarbodiimide (DCC), *N*-hydroxysuccinimide (NHS), dimethylformamide (DMF) and all buffer reagents were purchased from Sigma-Aldrich (France). CH_3O-PEG-SH (MW 2000 Da) was purchased from Rapp Polymere GmbH (Germany). EZ-Link NHS-biotin was purchased from Pierce Protein (Thermo Fischer Scientific, IL, USA). The buffer used for DNA aptamers spotting was a 1 M HK_2PO_4 solution, pH 9.25 while the one used for thrombin dilution, called Running Buffer, was 20 mM Tris–HCl, 1 mM $MgCl_2$, 120 mM NaCl, and 10 mM KCl, pH 7.4.

The oligonucleotides were purchased from Eurogentec (France) with a primary amine modification at the 5′-position (5′ Amino Modifier C6) and a 10-thymine spacer before the sequence of interest. These sequences are listed in Table 1. APT1c and APT2c correspond to the complementary strands of the sequences APT1 and APT2. They were used as negative controls for the detection of thrombin and positive control for the injection of biotinylated aptamers/amplification with SA. All chemicals were used without further purification.

Table 1
Oligonucleotide sequences.

Name	Sequence
APT1	5′-NH_2-T_{10}-GGT-TGG-TGT-GGT-TGG-3′
APT2	5′-NH_2-T_{10}-AGT-CCG-TGG-TAG-GGC-AGG-TTG-GGG-TGA-CT-3′
APT1c	5′-NH_2-T_{10}-CCA-ACC-ACA-CCA-ACC-3′
APT2c	5′-NH_2-T_{10}-AGT-CAC-CCC-AAC-CTG-CCC-TAC-CAC-GGA-CT-3′

2.2. DNA microarray fabrication

Oligonucleotides were grafted on gold-coated prisms (Horiba Scientific-GenOptics, France) as Self-Assembled Monolayers (SAM). First, a thiol functionality was introduced on the DNA oligonucleotides by conjugation with an activated NHS ester following a protocol inspired from Grosjean et al. (2005). 11-mercapto-undecanoyl-1-*N*-hydroxysuccinimide (HS-C11-NHS) was synthesised by mixing 1 M 11-mercapto-undecanoic acid, 1 M DCC and 1 M NHS in 10 mL of DMF. After overnight incubation under magnetic stirring, the solution was filtered through sintered glass and the filtrate was evaporated to dryness. Probe oligonucleotides (2 nmoles) functionalized with a primary amine group at their 5′-end were then conjugated to HS-C_{11}-NHS (160 nmoles) in PBS pH 8.0 for 1 h at room temperature. After purification by size exclusion chromatography (Illustra NAP-5 Columns kit, GE Healthcare) the purified HS-oligonucleotides were resuspended in HK_2PO_4 buffer and the DNA concentration was assessed by absorbance measurement at 260 nm.

The HS-oligonucleotides were arrayed on the gold surface of a glass prism by droplet deposition using a piezoelectric dispensing system (Siliflow, France). Before thiol SAM formation, prisms were cleaned by plasma treatment (0.6 mbar, 75% Oxygen, 25% Argon, power 40 W, 6 min) in a plasma generator (Femto, Diener Electronic, Germany) and droplets of approximately 4 nL HK_2PO_4 buffer containing a mixture of 10 or 20 μM thiol-modified DNA probes and 10 μM of methoxy-functionalised thiolated PEG (CH_3O-PEG-SH) were deposited by the droplet dispensing system under a controlled atmosphere of 85% humidity and left for 30 min to allow for a thiol mono-layer to auto-assemble on the surface. After overnight drying, prisms were thoroughly rinsed with deionised water and dried under an argon stream for few seconds. The size of the spots is approximately 500 μm with a separation of 1.25 mm between spots. The density of probes ranges from 5 pmol/cm^2 to 10 pmol/cm^2.

2.3. SPR imaging set-up

The detection of thrombin was monitored with a SPR imager (Scheme 1) apparatus (SPRi-Lab$^+$, Horiba Scientific-GenOptics) equipped with an incoherent light source (λ=635 nm). The reaction chamber consists of a hexagonal shape reactor (100 μm thick, 15 mm long and 9 mm wide) machined in a PEEK flow cell ($\approx$ 15 μL of volume). The flow cell was connected to PEEK tubing coupled with a degassing system (Alltech, France) and a syringe Cavro pump (Tecan, USA). The experiments were performed at 25 °C. All injections were dispensed using a 1 mL injection loop. Prior to the experiment, incubating a solution of 500 nM BSA and 500 nM cyt c diluted in running buffer for 1.5 h at room temperature blocked the biosensor surface. The SPR data were acquired using the software furnished by Horiba Scientific-GenOptics. Acquisition of the reflectivity signal, registered with a 12-bit camera, was initiated upon stabilization of the baseline. The reflectivity values were

averaged over the replicates of each spot and plotted upon time. In order to obtain the reflectivity shift upon binding of biomolecules, the initial reflectivity was subtracted from the raw data.

2.4. Thrombin real-time detection and sandwich formation

Series of injections were tested to study the kinetic formation of the sandwich complex (see Supplementary Data, Appendix A for the various injection protocols from P1 to P9). The secondary injected aptamer (either APT1 or APT2) was modified with a biotin at the 5′ end by conjugation with NHS-biotin using the same protocol as the conjugation with HS-C_{11}-NHS. The one-way flow rate of the Running Buffer was 50 μL/min.

Each thrombin injection (alone or in combination with other analytes) delivered 50 nM of protein diluted in Running Buffer and was dispensed via an alternating flow (15 μL dispensed volume, 10 μL aspirated volume, 50 μL/min flow rate). The injections were stopped after 30 min. Furthermore, a range of concentrations from 1 nM to 50 nM were also injected in order to determine the dissociation constants for both aptamers (see Supplementary Data, Appendix B).

To detect the sandwich formation, 8 min after the end of the thrombin injection, solutions containing either 100 nM APT1-bio alone or co-injected with 500 nM SA or 100 nM APT2-bio co-injected with 500 nM SA were loaded onto the DNA microarray with the same flowing parameters (back and forth mode for 30 min). The injection of 100 nM APT2-bio alone was carried by a one-way flow at 50 μL/min and lasted 10 min. When co-injected with an aptamer, the SA concentration was 5 times as much as the concentration of biotinylated aptamers to ensure complete complexation of soluble aptamers with SA. In contrast, when SA was loaded on the DNA microarray after completion of the reporter aptamer injections, the concentration was 50 nM with a flow rate of 50 μL/min. Finally, between each series of thrombin detection, the surface was regenerated by injection of a 1 M NaCl solution for 8 min at a flow rate of 50 μL/min to remove THR. If necessary, 50 mM NaOH was injected for 2–3 min to denature the hybridized complementary strands of DNA and regenerate the control spots.

3. Results

3.1. Thrombin detection from SPR imaging

Due to the advantages of real-time SPR imaging detection, it is possible to continuously monitor the interactions between thrombin and both aptamers APT1 and APT2 on a microarray. The injection of 50 nM thrombin (Fig. 1, Appendix A protocol P1) presents an association phase and a dissociation phase immediately following the injection of thrombin for each aptamer spot. A specific signal is observed on each spot containing either APT1 or APT2 aptamers while non-specific interactions on control spots (complementary sequences of aptamers and bare gold) were negligible. A range of concentrations from 1 nM to 50 nM (see Supplementary Data, Appendix B) confirms the label-free detection of thrombin with a detection limit as low as 1 nM with either APT1 or APT2 grafted on the surface of the biosensor. Furthermore, longer injections of thrombin were performed to reach equilibrium from which we deduced effective dissociation constants $K_D1 = 5.3 \pm 0.3$ nM and $K_D2 = 5.7 \pm 0.7$ nM for the binding of thrombin to grafted aptamers APT1 and APT2, respectively. These results are consistent with those obtained by Olmsted et al. (2011) for the solution phase interaction between thrombin and aptamers ($K_D1 = 5.96 \pm 0.57$ nM and $K_D2 = 3.86 \pm 0.68$ nM).

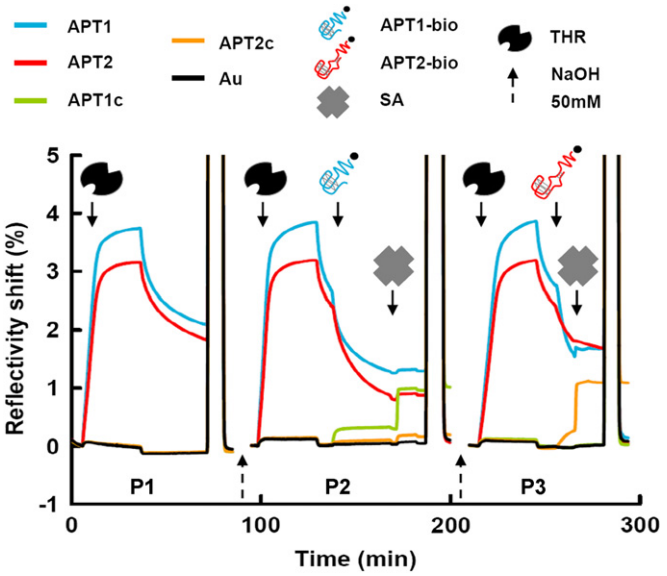

Fig. 1. SPR reflectivity shift after sequential injections of thrombin (THR), aptamer and streptavidin (SA) following protocol P1 to P3 (Supplementary Data, Appendix A). Between each protocol, regeneration is performed with 1 M NaCl injection. The arrows with dotted lines correspond to a further regeneration with 50 mM NaOH to remove the complementary DNA hybridized on control spots.

3.2. Sandwich formation after sequential injections of thrombin and the reporter aptamer

A second series of injections were performed in order to obtain the sandwich complex (Appendix A protocols P2 and P3). A secondary biotinylated aptamer (APT1-bio or APT2-bio) is injected as a reporter shortly after the end of the thrombin injection to ensure there is enough thrombin on the microarray for sandwich construction. Upon injection of APT1 or APT2, the respective control spots (APT1c or APT2c) give expected hybridization signals (Fuchs et al., 2010) thus confirming the accessibility of the surface immobilized DNA strands (Fig. 1). Furthermore, following injection of the reporter aptamer, the dissociation rate is increased on spots corresponding to the same aptamer due to displacement effects from thrombin bound to surface grafted aptamers towards free aptamers in solution. Surprisingly, instead of observing an expected increase in reflectivity corresponding to the reporter aptamer binding to thrombin bound on the alternative aptamer spots, an acceleration of the dissociation rate is also observed.

For a better comparison between the dissociation rates, the dissociation curves are expressed as the amount of complex remaining on the spot by a simple rescaling to 100% of the reflectivity at the initial time of the reporter aptamer injections (protocols P2 and P3) and after 8 min of Running Buffer injection with protocol P1 for comparison (Fig. 2). The lower dissociation rate is confirmed for the Running Buffer wash while the faster dissociation corresponds to the injection of the opposite aptamer on both aptamer spots. Different flow rates have been assayed to measure their possible influence on the recorded SPR responses. As no significant effect was observed, we used a flow rate of 50 μL/min for all injections. Several concentrations of aptamers in solution have also been tested and we found that concentrations above 100 nM yield similar results. For this reason, all injections of aptamer in solution were delivered at 100 nM.

In order to verify the presence of any sandwich complexes on the DNA microarray, SA is then injected to amplify the potential signal attributable to sandwich complexes. The SA is expected to bind to the biotin of the reporter aptamer. The control spots, APT1c or APT2c, confirm an efficient binding of SA on biotinylated

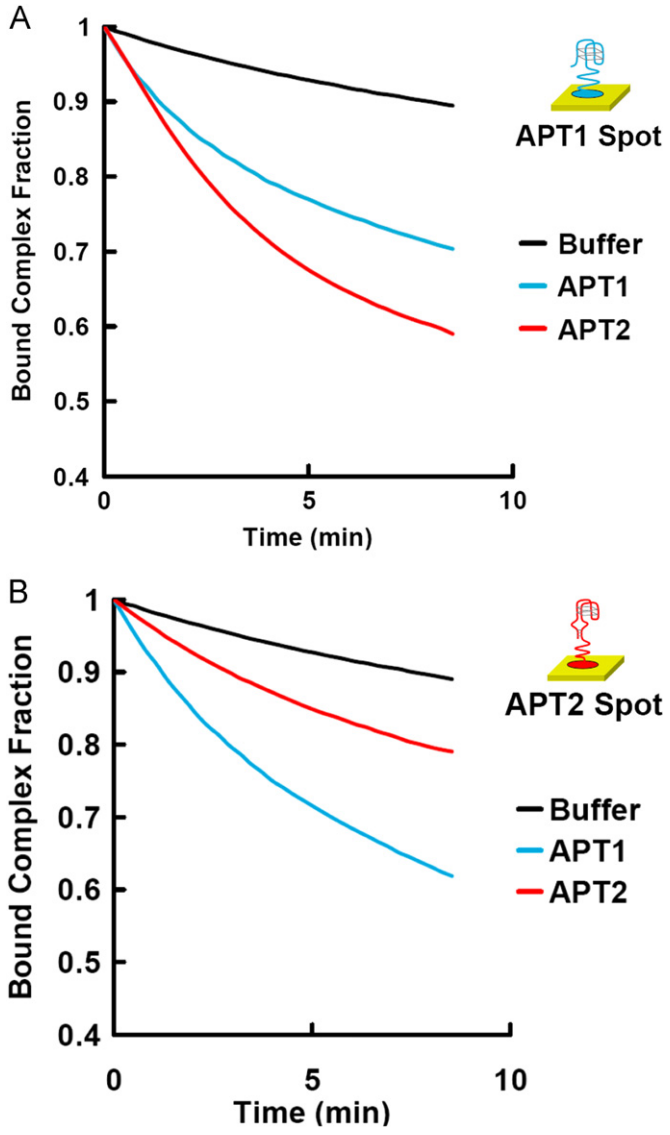

Fig. 2. Normalized thrombin dissociation kinetics after 8 min of running buffer wash and aptamer injection (A: APT1 spots and B: APT2 spots).

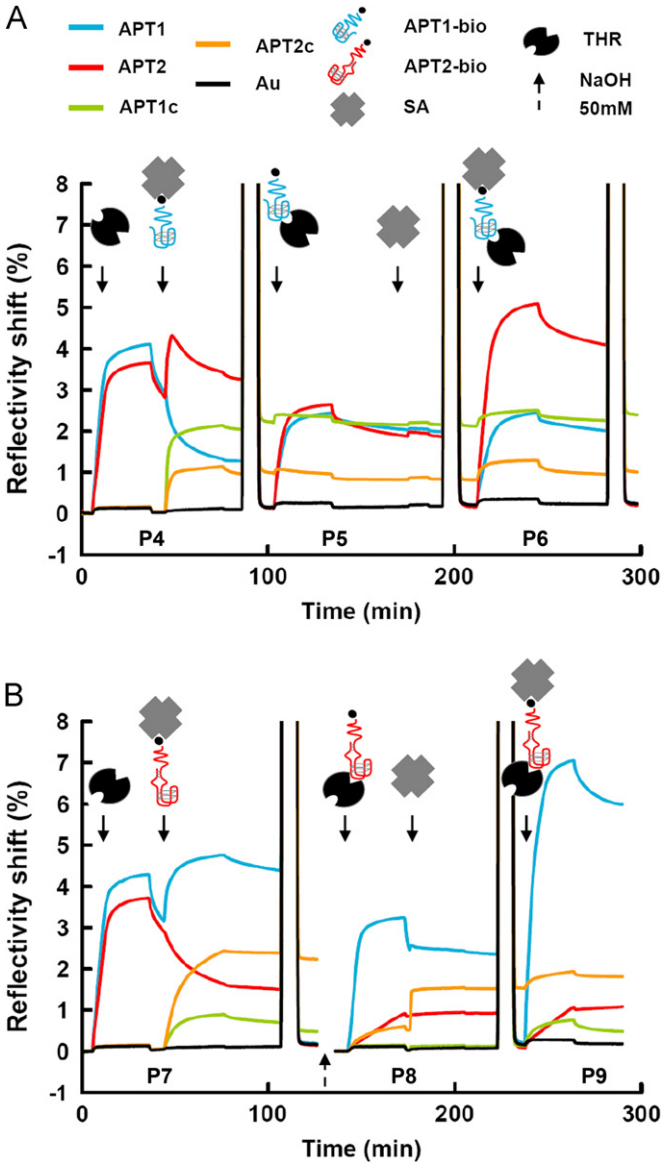

Fig. 3. SPR reflectivity shift for APT1 (A) and APT2 (B) injections following protocols P4 to P9 (Supplementary Data, Appendix A). The DNA microarray is regenerated between each protocol by NaCl washes. Further NaOH regeneration is indicated by an arrow.

reporter aptamers hybridized to their complementary strands. However, the SPR signal shifts on the aptamer spots, APT1 or APT2, do not show any adsorption of SA, enhancing the concerns about any sandwich formation on the biosensor. Similar results with unlabeled aptamers have been observed by Tang et al. (2007) without further explanation.

3.3. *Sandwich formation after co-injections of thrombin and the reporter aptamer*

Considering that the observation of trimeric complex formation is not possible upon sequential injection of each molecular element (thrombin, reporter aptamer and SA), we studied alternative strategies for the sandwich construction. These strategies, protocols P4 to P9 (Appendix A), are based on reducing the number of steps by co-injecting pre-assembled elements of the sandwich on the microarray (Fig. 3).

First, the injection of thrombin is followed by the co-injection of biotinylated aptamer pre-associated with SA (Appendix A protocols P4 and P7). Due to the molecular weight of the later complex, the SPR signal corresponding to the dissociation phase of the thrombin is counterbalanced by a signal increase due to the sandwich complex formation with SA-bound aptamers. This positive shift of SPR signal supports the presence of sandwich complexes with thrombin, aptamer and SA on the microarray when the injected aptamer is different from the grafted one (APT1 vs APT2). No amplification is observed on APT1 spots when APT1 is also used as a reporter aptamer leading to possible concerns on the APT1–thrombin–APT1 complex formation.

The co-injection of thrombin pre-bound to the biotinylated reporter aptamer is then tested, followed by an injection of SA for signaling purposes (Appendix A protocols P5 and P8). In this assay, the SPR signal shift is different depending on the nature of the secondary co-injected aptamer, APT1 or APT2. When the secondary aptamer pre-bound to thrombin is APT2-bio, similar responses are monitored than for the thrombin injected alone on the APT1 spot with only slightly lower equilibrium levels. In contrary, on APT2 spots, a strong reduction of the SPR reflectivity shift is observed. This is consistent with a large fraction of the injected thrombin already complexed with the APT2-bio aptamer in solution thus decreasing the concentration of thrombin with

free exosite II likely to interact with surface-grafted APT2 aptamers. On the other hand, when the aptamer pre-bound to thrombin is APT1-bio, the SPR signals on APT1 and APT2 spots are very similar -roughly as rapid as the one resulting from the injection of thrombin alone. The equilibrium level is only slightly lower than that for the thrombin injection alone. The pre-formed complex between thrombin and APT1 in solution does not seem to affect the further binding of thrombin on the APT1 spots of the biosensor. Furthermore, in both cases, co-injection of thrombin with either APT1 or APT2 followed by an injection of SA (Appendix A protocols P5 and P8), no significant SPR signal amplification is observed due to the SA binding to the biotin of the sandwich structure whereas the SA binding to biotinylated-aptamers hybridized on complementary strands of the control spots, APT1c or APT2c, presents a clear SPR signal increase.

Finally, simultaneous injections of thrombin, biotinylated aptamer (either APT1 or APT2) and SA are led on the DNA microarray (Appendix A protocols P6 and P9). The pre-assembling of the three molecular elements (protein–aptamer–SA) gives higher SPR signal increases than the sequential injection of one or two elements at the same time. As expected, the effect is more obvious on aptamer spots when the injection of the opposite aptamer is performed leading to a complex involving both exosites of thrombin with two different aptamers. On aptamer spots with similar reporter aptamer injection, no amplification are observed. However, whereas no or small SPR reflectivity shift is observed for thrombin, APT2-bio, SA co-injection on APT2 spots, the co-injection of thrombin, APT1-bio, SA present a significant signal increase on APT1 spot. Furthermore, the best signal amplification is observed for the co-injection of the three elements throbin, APT2 and SA on the APT1 spots (+7% of reflectivity shift).

3.4. Number of complexes formed on the biosensor

The real time kinetic data obtained from measurements of the SPR reflectivity shifts may be interpreted as the number of bound complexes. To this end, we use the proportionality between the reflectivity shift and the molecular mass deposited on the spots assuming the same refractive index for thrombin, SA and the aptamers. A simple rescaling of the association curves proportional to the Molecular Weight (MW) of the binding complex, either thrombin (protocol P1 in Fig. 1), thrombin–aptamer (protocols P5 and P8 in Fig. 3) or even thrombin–aptamer–SA (protocols P6 and P9 in Fig. 3) are presented on Fig. 4. The MW of the molecules are 36.7 K_Da for the thrombin, 8 K_Da for APT1, 12.3 K_Da for APT2 and 60 K_Da for SA. As can be seen from those MW, the binding of the reporter aptamer alone does not present a strong amplification of the SPR signal while the complex with SA may improve the observed signal by a factor 3 compared to the injection of thrombin alone. It is well known that Gold nanoparticles grafted with SA would further increase the amplification due to plasmonic behaviour (Kwon et al., 2012). However, no simple amplification factor could be obtained to quantitatively analyze the number of complexes formed on the different spots, thus the amplification with gold nanoparticles was not considered.

With this normalization procedure, it is thus possible to directly compare the number of complexed formed on the surface following the various protocols. To this end, we assumed that the complex is fully formed in solution before co-injection. This assumption is reasonable with the known values of the dissociation constants (in the range of nM) and the concentration of thrombin (50 nM) and aptamers (100 nM). We estimate that more than 90% of the thrombin is complexed with the aptamers. While SA is also co-injected, the low dissociation constant (K_D~fM) for the biotin–SA complex guarantees the complete formation of the aptamer–SA complex.

Fig. 4A presents results obtained from APT1 spots with an obvious reduction in the number of injected complexes (either

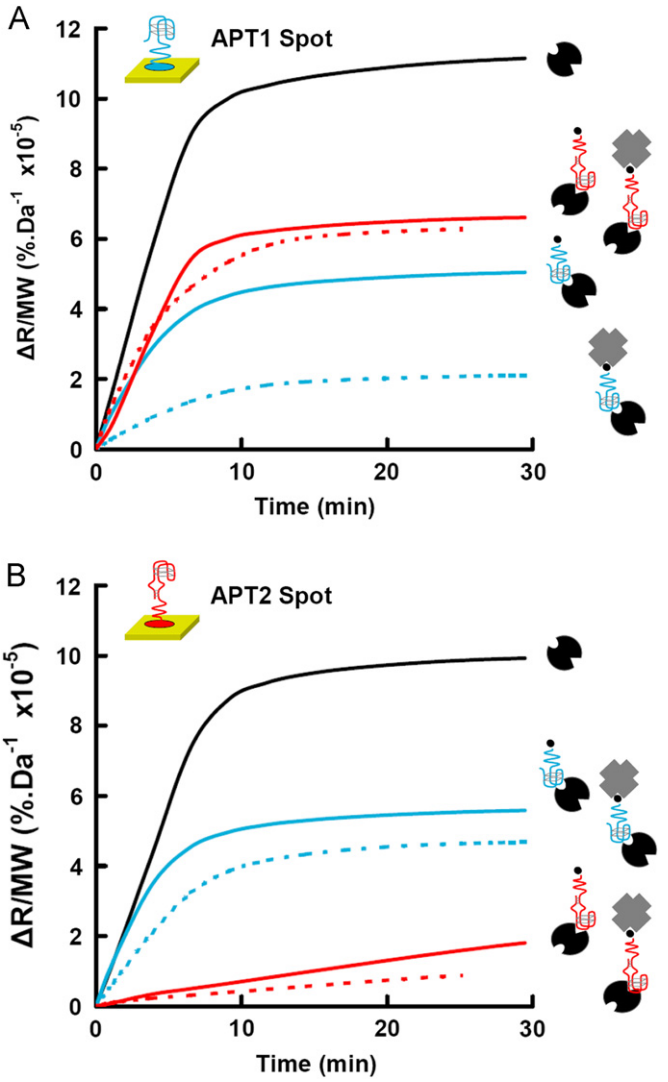

Fig. 4. SPR reflectivity shifts normalized by the molecular weight of the injected complex observed on APT1 spots (A) and APT2 spots (B) to count for the number of complexes bound to the biosensor. Various injections are considered: free thrombin, aptamer complexed with thrombin and trimeric complex (thrombin, biotinylated aptamer and streptavidin).

thrombin–aptamer or thrombin–aptamer–SA) bound to the surface compared to the amount of thrombin bound when injected alone. For thrombin–APT2 and thrombin–APT2–SA complex injections, a similar amount of complex bound is observed and corresponds to 50–60% of the amount of thrombin bound upon injection alone. The similar results obtained for both dimeric and trimeric complexes confirm the adsorption in a sandwich format. More surprisingly, the signals given by the thrombin–APT1 and thrombin–APT1–SA complexes differ by at least a factor of 2. This suggests the presence of thrombin on the APT1 spot but questions the complete formation of either APT1–thrombin–APT1 or APT1–thrombin–APT1–SA complexes. In fact, the ratio between the signals observed following both co-injections is compatible with only thrombin binding to the APT1 spot.

Results for APT2 spots presented in Fig. 4B are compatible with the expected binding of the full complex when the APT1 is co-injected and with the expected absence of complex formation when APT2 is co-injected. The slow and linear increase of the SPR signal shift for the APT2 co-injections is similar to the signal obtained for free thrombin in solution at a reduced concentration of 5 nM or lower (see Supplementary Data, Appendix B). This

confirms the estimate of less than 10% of free thrombin present in solution when co-injected with APT2. As for the APT1–thrombin–APT2(–SA) complex on APT1 spots, only 50 to 60% of the APT2–thrombin–APT1(–SA) complex seems to be formed on APT2 spots compared to the amount of thrombin bound after the injection of thrombin alone.

4. Discussion

4.1. Selectivity of the aptamers towards thrombin exosites

The existence of two potential binding sites on the thrombin asks for the selectivity of the two aptamers APT1 and APT2 towards these exosites. From the injection of bound thrombin–APT2 and the resulting low level of SPR signal on APT2 spots, it seems evident that the second aptamer APT2 presents a strong selectivity towards a single binding site, the exosite for the heparin (Tasset and Kubik, 1997). In contrast, the pronounced signal observed following the APT1–thrombin complex injection suggests the possibility for APT1 to bind both thrombin exosites. Further evidences are brought by the existence of sandwich construction with only APT1 for amplification purposes in thrombin detection assays (Bai et al., 2011; Ding et al., 2010; Li B. et al., 2008; Wang et al., 2011). The cross-reactivity of APT1 with both exosites may significantly interfere with the propensity of sandwich formation. Consequences for the amplification protocols are important as we will discuss later. It also reveals the misleading definition of a single K_D for the APT1 interaction with thrombin as two different dissociation constants should in fact be defined corresponding to the binding of APT1 with each exosite. The measurement of a single effective K_D1 actually involving two interactions may explain most of the variability observed in the data published depending on the experimental techniques considered.

A possible explanation for the difference in selectivity towards thrombin exosites for the two aptamers may be found in their secondary structures. They both present a G-quadruplex whereas additional dangling ends for the second aptamer APT2 form a small duplex. Recently, this duplex has been shown to play a role in the binding with thrombin (Lin et al., 2011). Minute structural difference along with a longer DNA sequence may explain the higher selectivity of APT2 towards thrombin exosites as compared to APT1.

4.2. Assessment of the possible allosteric effect upon sandwich complex formation

Various studies have considered the possible allosteric effect in reactivity of thrombin with its natural ligands (Fredenburgh et al., 1997; Verhamme et al., 2002). Far fewer studies have considered the possible allosteric effect of aptamers upon binding to thrombin and the subsequent impact on the sandwich formation of the complex. Olmsted et al. (2011) have recently determined the dissociation constants for all possible binding reactions: APT1 and APT2 binding to a free thrombin (K_D1 and K_D2, respectively) but also APT1 binding to the APT2–thrombin complex (K_D3) and APT2 binding to APT1–thrombin (K_D4). Unexpectedly, Olmsted et al. (2011) observed differences in dissociation constants for free or aptamer bound thrombins with lower K_D for bound thrombin ($K_D3 < K_D1$ and $K_D4 < K_D2$). Based on those results, the sandwich formation should be favoured since the formation of the second interaction of an opposite aptamer with thrombin pre-bound to a grafted aptamer is improved compared to the same interaction with free thrombin.

Surprisingly, we observed a destabilisation of any pre-formed complex made of thrombin bound to surface-grafted aptamer when the alternative aptamer was injected on the sensor (protocols P2 and P3 in Fig. 1). This is particularly evident in Fig. 2 where dissociation rates of the bound thrombin are presented upon injection of the Running Buffer alone or upon aptamer injections. In both cases, thrombin bound to APT1 or APT2, the lowest dissociation rate is for Running Buffer injection alone while the fastest one corresponds to the injection of the opposite aptamer in solution. The lowest rate with Running Buffer alone may be explained by possible multiple binding of thrombin on the surface since the unbound thrombin is slowly washed off and a non negligible concentration of thrombin at the surface may be present. Increased flow rate is known to correct this effect, but no substantial effects were observed even at 250 μL/min (5 times the usual flow rate). It may also be solved by injection of the free probe in solution to compete with the grafted probe for thrombin binding. In this respect, the faster dissociation rates observed when the same aptamer as the grafted one is injected illustrate this competition effect. However, the fastest rate for injection of the opposite aptamer may not only be explained by this competition effect. A further destabilization of the thrombin–aptamer complex upon binding of an aptamer to the opposite exosite is involved. Such results are obtained whatever the aptamer (APT1 or APT2) used and contradict a possible positive allosteric effect presented by Olmsted et al. (2011). In fact, their results unambiguously present thermodynamical contradictions. The equilibrium cycle leading to APT1–thrombin–APT2 via the APT1–thombin or the APT2–thrombin alternative paths would suggest $K_D1\ K_D4 = K_D2\ K_D3$. Unfortunately, this is in explicit contradiction with their results since $K_D1\ K_D4 = 11.3 \pm 2.3\ \mathrm{nM}^2$ and $K_D2\ K_D3 = 3.34 \pm 1.3\ \mathrm{nM}^2$. The binding of APT1 to both exosites of the thrombin may explain this thermodynamical inconsistency. K_D1 may only be seen as an effective dissociation constant while a rigorous analysis should define two different dissociation constants for APT1 to the free thrombin depending on the binding site. Thus, the positive allosteric effect observed by Olmsted et al. (2011) may be questioned and may reveal difficulties in the sandwich complex formation brought by the non-selectivity of APT1 towards thrombin exosites.

4.3. Choice of the best amplification protocol for the sandwich complex formation

From the insights on the kinetic formation of the sandwich complex between two aptamers and thrombin, we aim to provide the best strategy for amplification strategy in diagnostic assays. In this respect, we have confirmed that successive injections of thrombin, secondary aptamer and reporter or amplification molecules (protocols P2 and P3 in Fig. 1) would only form a small number of complete sandwich complexes on the biosensor that are not visible using SPR detection. However, we obtained such sandwich complex formation upon co-injection of aptamer-reporter (i.e., aptamer pre-bound to SA) following the previous thrombin injection (protocols P4 and P7 in Fig. 3) and with even more amplification for co-injection of thrombin, aptamer and SA (protocols P6 and P9 in Fig. 3). The sandwich is principally formed on the aptamer spots when the opposite aptamer is injected leading to APT1–thrombin–APT2 complex. It is however important to note that only half of the full sandwich complexes are formed compared to the number of bound thrombin when injected alone (Fig. 4). This seems principally related to the fact that the binding of an aptamer to an already bound thrombin is less efficient than to free thrombin (negative allosteric effect).

Furthermore, no APT2–thrombin–APT2 sandwich has been observed and serious concerns about the effective formation of APT1–thrombin–APT1 exist. This is particularly evident when comparing results for APT1–thrombin–APT1 complex formation and APT1–thrombin–APT1–SA on Fig. 4A. The lower level for the latter is related to the presence of thrombin alone on the spots and not in association with the injected APT1 and the reporter molecules. In addition, absence of the reporter molecules

in the complex formed on the biosensor does not allow end-point detection.

Finally, when considering the APT1–thrombin–APT2 sandwich, it is interesting to compare the results for the choice of the aptamer grafted to the biosensor. From our results (Fig. 3), grafting APT1 seems the best strategy since it corresponds to the highest increase in the SPR signal (7% of reflectivity shift). This characteristic was expected due to the binding ability of APT1 towards both exosites. The co-injection of thrombin and APT2 leaves one exosite of the thrombin free for further binding to grafted APT1. On the contrary, while co-injecting APT1 and thrombin, the possible binding of APT1 to exosite II reduces the amount of thrombin accessible for further binding to the biosensor on the grafted APT2.

5. Conclusion

The label-free and real-time kinetics detection by SPR imaging technique allows us to evaluate various protocols for the sandwich formation between thrombin and its aptamers. In particular, we confirmed the binding of APT1 on both exosites of thrombin and the selectivity of the APT2 towards the heparin binding site. The multiple binding sites of APT1 to thrombin allow a sandwich complex formation with two APT1 strands (APT1–thrombin–APT1) as previously reported (Bai et al., 2011; Ding et al., 2010; Li et al., 2008; Wang et al., 2011) though we have not confirm this sandwich formation using kinetics analysis. The best strategy for signal amplification requires the pre-incubation of thrombin with one aptamer and the amplification reporter in solution before the injection on the biosensor, which seems to favour the complex with both aptamers (APT1–thrombin–APT2). Due to the low selectivity of APT1 towards thrombin exosites, a preference for APT1 as the grafted aptamer is evident implying a co-injection of thrombin with APT2. In conclusion, the sandwich complex formation would be greatly improved by the existence of a selective aptamer towards the fibrinogen exosite considering that APT2 already presents this selectivity towards the heparin exosite. In fact, the thrombin–APT2 complex may allow the selection of this new aptamer, as only the expected binding site is free to interact.

Appendix A. Supporting information

Supplementary data associated with this article can be found in the online version at http://dx.doi.org/10.1016/j.bios.2012.07.016.

References

Ahmad, K.M., Oh, S.S., Kim, S., McClellen, F.M., Xiao, Y., Soh, H.T., 2011. PloS One 6, e27051.
Bai, L., Yuan, R., Chai, Y., Yuan, Y., Zhuo, Y., Mao, L., 2011. Biosensors and Bioelectronics 26, 4331–4336.
Bock, L.C., Griffin, L.C., Latham, J.A., Vermaas, E.H., Toole, J.J., 1992. Nature 355, 564–566.
Centi, S., Tombelli, S., Minunni, M., Mascini, M., 2007. Analytical Chemistry 79, 1466–1473.
Chen, Q., Tang, W., Wang, D., Wu, X., Li, N., Liu, F., 2010. Biosensors and Bioelectronics 26, 575–579.
Ding, C., Ge, Y., Lin, J.-M., 2010. Biosensors and Bioelectronics 25, 1290–1294.
Ellington, A.D., Szostak, J.W., 1990. Nature 346, 818–822.
Fredenburgh, J.C., Stafford, A.R., Weitz, J.I., 1997. Journal of Biological Chemistry 272, 25493–25499.
Fuchs, J., Dell'Atti, D., Buhot, A., Calemczuk, R., Mascini, M., Livache, T., 2010. Analytical Biochemistry 397, 132–134.
Grosjean, L., Cherif, B., Mercey, E., Roget, A., Levy, Y., Marche, P.N., Villiers, M.-B., Livache, T., 2005. Analytical Biochemistry 347, 193–200.
Jayasena, S.D., 1999. Clinical Chemistry 45, 1628–1650.
Kwon, M.J., Lee, J., Wark, A.W., Lee, H.J., 2012. Analytical Chemistry 84, 1702–1707.
Lane, D.A., Philippou, H., Huntington, J.A., 2005. Blood 106, 2605–2612.
Li, Y., Guo, L., Zhang, F., Zhang, Z., Tang, J., Xie, J., 2008. Electrophoresis 29, 2570–2577.
Li, B., Wang, Y., Wei, H., Dong, S., 2008. Biosensors and Bioelectronics 23, 965–970.
Lin, P.-H., Chen, R.-H., Lee, C.-H., Chang, Y., Chen, C.-S., Chen, W.-Y., 2011. Colloids and Surfaces B: Biointerfaces 88, 552–558.
Olmsted, I.R., Xiao, Y., Cho, M., Csordas, A.T., Sheehan, J.H., Meiler, J., Soh, H.T., Bornhop, D.J., 2011. Analytical Chemistry 83, 8867–8870.
Sassolas, A., Blum, L.J., Leca-Bouvier, B.D., 2011. Biosensors and Bioelectronics 26, 3725–3736.
Tang, Q., Su, X., Loh, K.P., 2007. Journal of Colloid and Interface Science 315, 99–106.
Tasset, D., Kubik, M., 1997. Journal of Molecular Biology 272, 688–698.
Tennico, Y.H., Hutanu, D., Koesdjojo, M.T., Bartel, C.M., Remcho, V.T., 2010. Analytical Chemistry 82, 5591–5597.
Tombelli, S., Minunni, M., Mascini, M., 2005. Biosensors and Bioelectronics 20, 2424–2434.
Tuerk, C., Gold, L., 1990. Science 249, 505–510.
Verhamme, I.M., Olson, S.T., Tollefsen, D.M., Bock, P.E., 2002. Journal of Biological Chemistry 277, 6788–6798.
Wang, J., Zhu, Z., Munir, A., Zhou, H.S., 2011. Talanta 84, 783–788.